An Introductory CFD Analysis Study of Novel Cavity Vane Driven Wind Turbine Blade Design

S.N. Ashwindran, A.A. Azizuddin, A.N. Oumer*
Faculty of Mechanical and Automotive Engineering Technology,
Universiti Malaysia Pahang, Malaysia
**azizuddin@ump.edu.my*

Azli Abd Razak
Faculty of Mechanical Engineering
Universiti Teknologi MARA (UiTM), Shah Alam, Malaysia

ABSTRACT

Climate in Malaysia is heavily influenced by monsoon seasons, where the wind speed pattern is inconsistent and highly unsteady. Existing commercial wind turbines are only designed to accommodate high wind speed regions. In order to harvest energy in Malaysia, design modification is required on conventional wind turbine blade. This paper presents an introductory computational investigation of proposed drag driven vertical axis wind turbine. The objective of this research is to investigate the factors that govern the aerodynamics attributes of the proposed design. The design is simulated in 2D using sliding mesh technique via FLUENT based on URANS model. Previous mesh dependency study shows that fine and medium grid topology indicated a good agreement. In this numerical study, the proposed wind turbine is simulated based on SST k-ω turbulent transport model under fine grid spatial discretization. The design is analyzed under the influence of constant freestream velocity of 25 m/s in order to study the behavior of the turbine at high speed and low RPM. Result shows that high static pressure of 64.8 kPa exerts on the returning blade 1 which overwhelms the motion of advancing blade. Blade 1-3 indicated stable numerical values after 216°. Hence, the governing factors in terms of flow properties that affected the wind turbine are studied for future improvement. It is found that the cavity vane of the proposed design requires modification in order to improve moment.

Keywords: *Vertical Axis Wind Turbine, CFD.*

ISSN 1823-5514, eISSN 2550-164X

Received for review: 2020-03-18
Accepted for publication: 2020-09-17
Published: 2020-10-15

Introduction

Wind turbines (WT) are categorized into two types relative to their axis of rotation namely vertical and horizontal axis. In commercial perspective horizontal axis wind turbine (HAWT) are the most preferred by the industry players in contrast to vertical axis wind turbine (VAWT) [1]. However, VAWT is more suitable for energy harvesting in urban and low speed wind potential areas [2]. VAWT holds several advantages over HAWT namely: omnidirectional without the need of yaw mechanism [3], less noise [4], efficient in turbulent environments [5], and easier to incorporate into buildings [6]. In Malaysia wind related technologies are not celebrated as other renewable energy resources which can be seen by the lack of support from Malaysian government by not providing feed in tariffs (FiT) for wind power [7, 8]. In terms harvesting wind energy in Malaysia, offshore wind facilities indicate promising prospect than onshore [9, 10]. Siti Khadijah [11] stated that during monsoon season wind speed of offshore point in east coast region of Malaysia can reach up to 15 m/s. Moreover, wind speed can reach up to 10 m/s at the offshore regions of Sabah and Sarawak due to the influence of typhoon occurrence at Philippines [12]. This clearly indicates that offshore wind speed is adequate for energy harvesting in comparison to onshore region in Malaysia. However, wind speed in Malaysia is highly influenced by monsoon seasons thus making the wind speed inconsistent and highly unsteadies [13].

Current existing WTs are designed to accommodate wind speed relative to high wind speed regions namely Denmark, India, United States, China and others [7, 8]. Hence, design modification and improvement are implemented on WT design in order to improve the effectiveness in harvesting wind energy at low, unsteady and inconsistent wind speed region. Hence, a novel drag driven wind turbine design at vertical axis configuration is proposed for offshore region of Malaysia. The proposed design is simulated under the influence of constant freestream velocity of 25 m/s as cut off speed in order to study the behavior at high wind speed. The aim of the research is to investigate the factors that govern the aerodynamics attributes of the proposed design. The simulations were carried out in ANSYS-Fluent in 2D configuration using unsteady Reynolds-Averaged Navier Stokes (URANS) as the numerical strategy in computing the flow field properties.

Computational Methodologies

Model geometry configurations

The presented geometry was generated by combining three different size of novel cavity vane shape which is composed of different geometric parameter. The proposed design consists of three blades configured at 120° apart from

each blade. The design parameters such as aspect ratio (AR) and swept area (S_A) are numerated using Equation 1-2 relative to VAWT design parameter. The proposed turbine has an aspect ratio (AR) of 0.5, swept area (S_A) of 190 m^2, rotor diameter (D_r) of 19 m and blade height (H) of 10 m. For simplicity, the 2D planar section of the design which represents the blade bend is selected for study. The plane is 4 m (H_p) from the datum as shown in Figure 1.

$$AR = \frac{H}{D_r} \tag{1}$$

$$S_A = D_r \times H \tag{2}$$

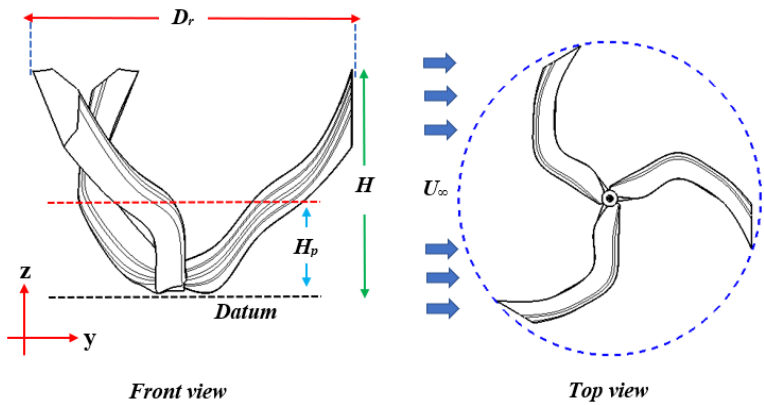

Figure 1: Proposed wind turbine design configuration.

Figure 2(a) shows the design parameter of the cavity vane used to construct the proposed wind turbine. The cavity vane consists of three primary edge fillets denoted as R2, R3, and R4. The thickness (t) of the cavity vanes are 0.2 m. Table 1 shows the geometric attributes of the cavity vane A, B and C. Three of the cavity vanes share the similar dimensions with regards to primary edge fillet. However, the varying factors of the cavity vanes are the angle of twist, radius (J) and width (K). The cavity vane sections are joined at an angle (α) of twist of 25° at vane profile A and C. Meanwhile R1 and R5 represent the blade curvature of the cavity profile. Figure 2(b) shows the resulted blade morphology by the combination of the cavity profile at different parametric configuration.

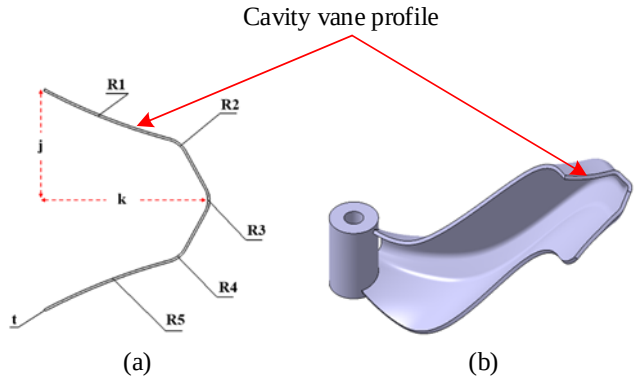

Figure 2: Blade profile: (a) Cavity vane design parameter (b) blade morphology.

Table 1: Geometric attributes of cavity vane

Cavity vane (A)	Value	Cavity vane (B)	Value	Cavity vane (C)	Value
R_1, R_5	6 m	R_1, R_5	6 m	R_1, R_5	6 m
R_2, R_4	0.24	R_2, R_4	0.24 m	R_2, R_4	0.24 m
R_3	0.4 m	R_3	0.4 m	R_3	0.4 m
K	0.8 m	*K*	1.6 m	*K*	2 m
J	0.5 m	*J*	1 m	*J*	2 m
α	25º	α	0º	α	25º
t	0.2 m	*t*	0.2 m	*t*	0.2 m

Computational configurations

The presented design is highly asymmetrical due to blade curvature and variation in cavity vane structure. Consequently, conducting CFD analysis in 3D configuration will incur large computational load then in 2D regardless the numerical strategies and spatial discretization being utilized. Moreover, the proposed design is at initial stage of research, hence CFD investigation in 2D configuration is deemed sufficient. The 2D WT is configured in a virtual wind tunnel domain (main domain) as illustrated in Figure 3(a). The virtual wind tunnel domain consists of two mesh configurations. Static and moving mesh domains are denoted as steady domain and rotating domain respectively. The WT is simulated under finite volume method (FVM) discretization based on URANS strategy. There are several robust numerical strategies in computing flow fields which are categorized according to the consumption on computational load and appropriateness to the case study

and governing factor. Researcher widely utilize URANS model in CFD analysis due to the low computational cost and does not require high quality grid resolution [16].

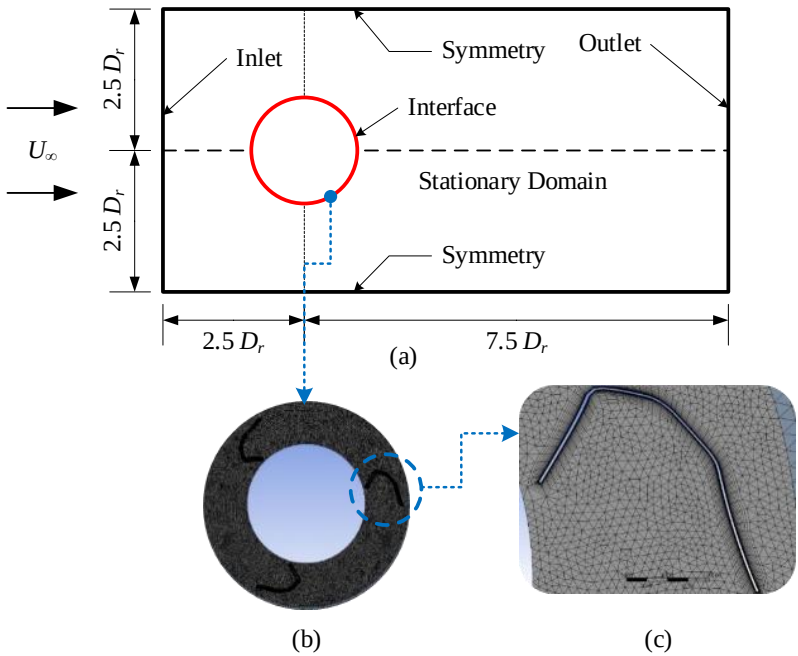

Figure 3: Domain configurations: (a) main-steady domain configuration and dimension, (b) rotating domain, (c) inflation layer around blade region.

Boundary condition

The WT is simulated under Neuman boundary condition at constant freestream velocity. As displayed in Figure 3(a), the steady domain consists of an inlet assigned to receive freestream velocity of U_∞ = 25 m/s in the +x-direction from left. The side walls of the steady domain are assigned as symmetry with free slip condition. The outlet is set to zero pascal gauge pressure. The blade wall is set to no slip condition. The rotating zone is initiated to rotate at 40 RPM. Meanwhile, the computational domains are constructed and partitioned relative to Dr dimension as shown in Figure 3(a). Commonly, researcher constructs large sized domains to ensure the consideration of far-field properties and also to accurately capture flow field properties. However, in this study the domains are constructed relatively smaller than the conventional domain in order to save computational time.

Sliding mesh technique is employed on the rotating domain for mesh motion. Previous mesh sensitivity study illustrated trivial difference between fine and medium mesh resolution [21, 22]. Therefore, fine mesh configuration is chosen. Figure 3(b) and 3(c) show the mesh topology around the blade region. Non-conformal mesh method is used for spatial discretization of steady and rotating domain to ensure non-connectivity between the nodes of the domain. The steady domain is generally composed of triangular mesh. Rotating domain is discretized with triangular mesh type with smaller face size than steady domain. The blades of the turbine are composed of 17 inflation layers with 1.2 growth ratio based on smooth transition method.

Based on literature survey, SST k-ω turbulent transport model is widely preferred by researcher to perform numerical study on WT performance [19]. The turbine is computed in 2D planar space at transient incompressible flow configurations. Coupled scheme is used in pressure-velocity coupling computation where the spatial discretization for turbulent kinetic energy and specific dissipation rate is set to set second order upwind. The convergence criteria of residual imbalance are set to 10-5. Since actual or experimental data on turbulent parameters control such as turbulent intensity and viscosity are not available, the controls on turbulent parameters are set based on assumption for high turbulent intensity or high-speed flow which is 5% for turbulent intensity and 10 % for turbulent viscosity. Meanwhile, Courant-Friedrichs-Lewy (CFL) number is set to 10. Although the recommended range CFL number is from 0.5-1, factors of CFL is not taken into major criteria since low CFL number increases the computational time. The time-step size is set to 0.01 with 25 iterations per timestep. Table 2 reports the simulation configurations.

Table 2: Boundary condition parameters

Boundary condition	Parameter	Value
Boundary condition type	Neuman	-
Inlet	Constant	U_∞ = 25 m/s
Outlet	-	0-Gauge pressure
Bounding wall	Symmetry	Free-slip condition
Blade wall	Shear condition	No-slip condition
Turbulent intensity	-	5 %
Turbulent viscosity	-	10%
Turbulent scheme	Second order upwind	-
Pressure -velocity coupling scheme	Coupled scheme	-

Numerical performance parameters

Wind turbines can be analyzed by numerically analyzing key parameters that dictates the aerodynamic and mechanical performance as illustrated in Equation 3-5. Such parameters are tip speed ratio (*TSR*) and power extraction coefficient (C_p).

Moment coefficient:

$$C_m = \frac{M}{\frac{1}{2}\rho U_\infty^2 D_t} \tag{3}$$

Drag coefficient:

$$C_D = \frac{F_D}{\frac{1}{2}\rho S_A U_\infty^2} \tag{4}$$

Tip speed ratio:

$$TSR = \frac{\omega \times \left(\frac{D_r}{2}\right)}{U_\infty} \tag{5}$$

Tip speed ratio is a crucial parameter in analyzing power extraction. The power extraction coefficient, C_p values are numerated with regards to TSR using Equation (6).

$$\Delta C_p = \Delta C_m \times TSR \tag{6}$$

CFD Numerical Results

Figure 4 shows the drag coefficient of individual blades. The graph indicates the oscillating response of the blade relative to the angular position to the upstream velocity. As manifested in Figure 4 and 5, blade 3 experience a sheer drop of drag coefficient and rise of lift coefficient. Meanwhile it is noted that blade 2 is driven by drag force at the initial stage of rotation. As illustrated in Figure 6, blade 3 experiences drop in moment coefficient due to declining drag coefficient. However, it is observed that blade 2 experiences rise in lift and drag coefficient, consequently increasing the moment coefficient in blade 2.

Average Y^+ by surface integrals value under facet average via turbulent field variable indicated 35.27, in which falls under the category of log-law region. Although it is highly recommended for Y^+ value for SST turbulent model to be less than 1 at preliminary stage of research it is deemed sufficient.

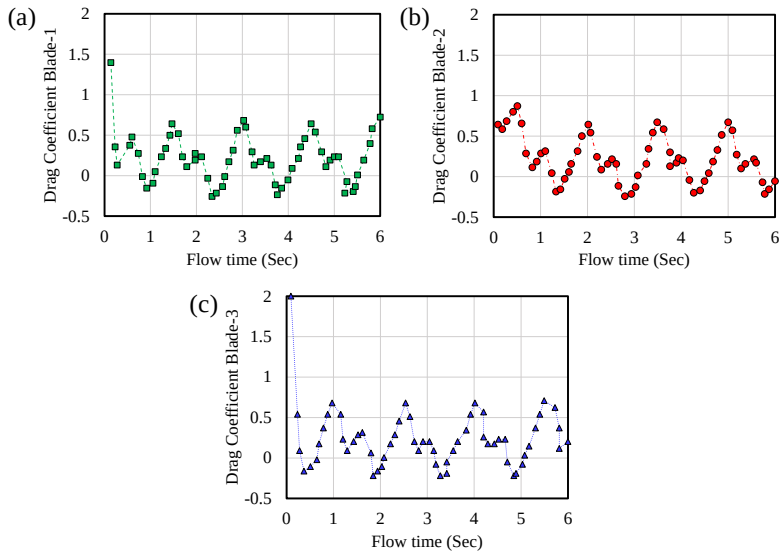

Figure 5: Drag coefficient against flow time for (a) blade 1, (b) blade 2 and (c) blade 3.

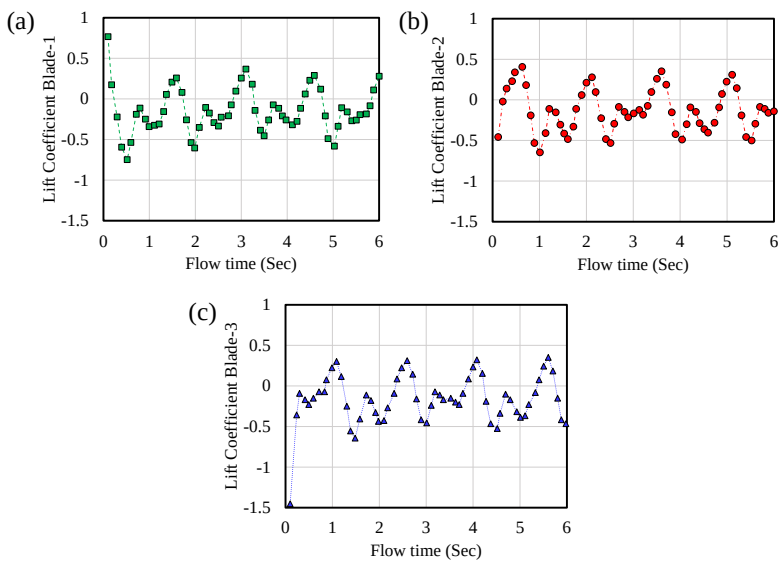

Figure 5: Lift coefficient against flow time for (a) blade 1, (b) blade 2 and (c) blade 3.

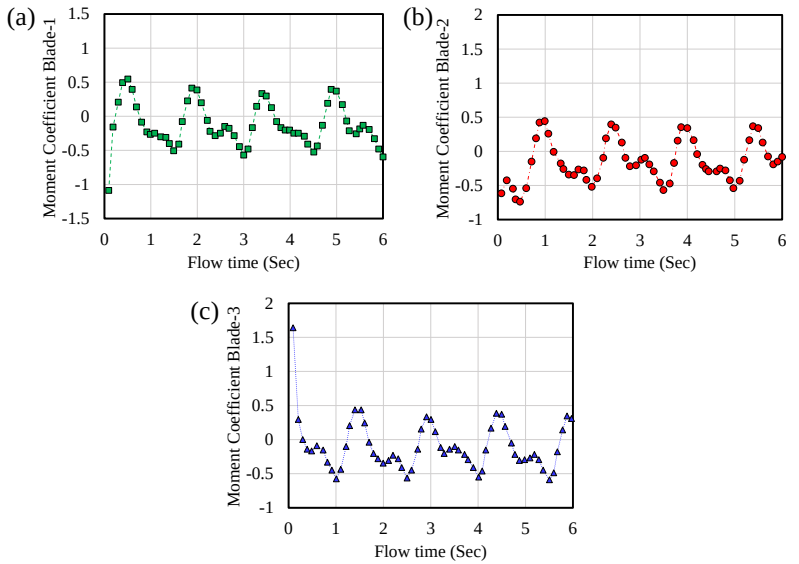

Figure 6: Moment coefficient against flow time for (a) blade 1, (b) blade 2 and (c) blade 3.

Figure 7 displays the aerodynamics results of blade 1, 2 and 3 of drag, lift and moment magnitude against azimuth angle. The results show that blade 3 at 0° azimuth angle generates the highest drag force FD of 11.08 kN, resulting in high positive moments of M = 9.03 kN/m and lowest lift force FL of 7.97 kN. At this orientation, the moment values are dominated by drag forces and the lift forces has minimal contribution to moment generation. This is due to the orientation of the blade 3 facing upwind direction, therefore it requires high drag forces and moment to initiate rotations because of the size and drag induced geometry design. After 24° it is noticed that blade 3 has a shear drop of drag forces due to the effect caused by the returning blade 1 resulting in negative moment and drag forces. After 216° the drag forces start to increase due to the increase of lift forces which are assisted with the transition of moment which increases from negative values. Moment generation for blade 3 starts to stabilize into smooth periodic oscillation after 312° with stable numerical values. Blade 3 reaches the highest moment at 336° after the initial values and lowest at 240°. Blade 2 achieves lesser results because of orientation with regards to wind direction. Blade 2 indicates stable periodic oscillation after 312°. Meanwhile for blade 1 at 0° orientation the polynomial convex shape faces the opposite to wind direction which explains the generation of negative moments and high drag forces in comparison to polynomial concave blade 3 facing the upwind direction.

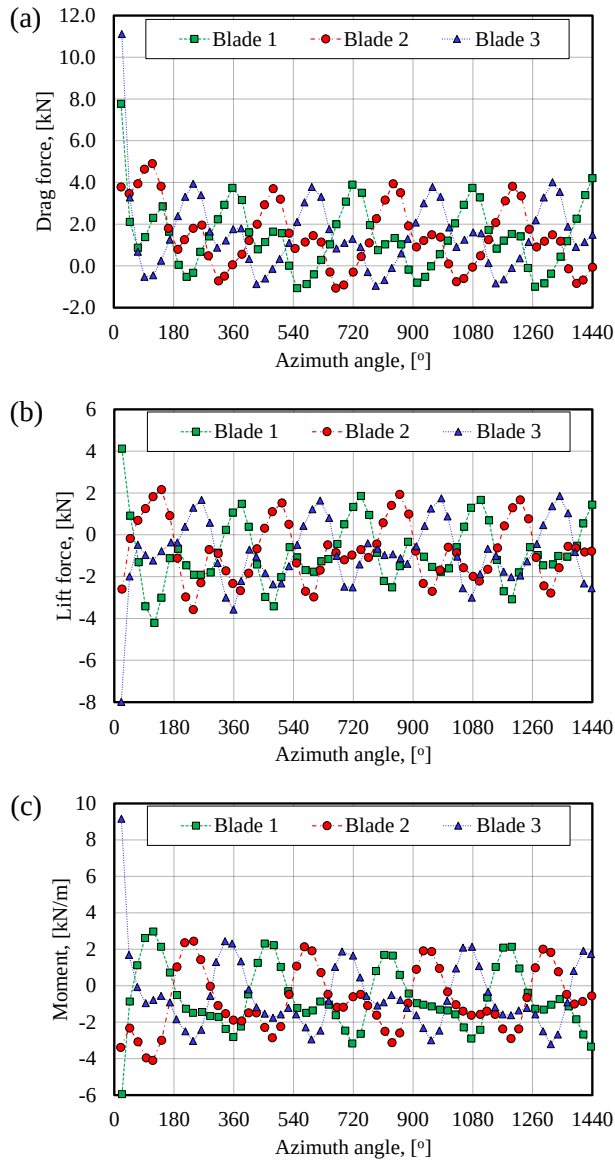

Figure 7: Aerodynamic forces against Azimuth angle. (a) drag force, (b) lift force and (c) moment.

Figure 8 presents the pressure contour result of blade regions at different azimuth angle of four complete revolutions of 24°, 360°, 720° and 1080°. The result indicates high static pressure at 24° of blade 1 as a result of high adverse pressure gradients which contribute to negative moment due to dynamic stall. Therefore, it requires high drag force and pressure for blade 3 to generate positive moment due to negative moment cause by returning blade 1. As the revolution continues the adverse pressure gradient reduces since the turbine starts to gain momentum and inertia in blade 3 and blade 2 regions. High static pressure regions are still noticeable around blade 1 due to the configuration issue experienced by drag-induced VAWT commonly known as self-starting issue or 'dead band' [24, 25]. Between $180° < \theta < 1440°$, the moment generation decrease to a smaller stabilized value which is due to Betz limit the maximum amount of kinetic energy can be extracted by turbine from flowing wind. As displayed in Figure 9 the generated streamline indicates a strong wake region downstream of the turbine causing it to generate strong vortex shedding region. In principle the intensity of wake region is depended on the geometry induced to a flow stream. Since it is a drag type WT without streamline properties it is sensible to notice high wake regions. The wake regions are generated due to flow losing momentum after excreting forces on the corresponding body. The steep high static pressure gradient induced by the geometry resulted in flow separation and vortex shedding downstream of the turbine caused by drag force along the blades region. It is noted by several research that strong vortex shedding and wake region will result in low torque contribution. In the influence of design geometry, high pressure region is noticed on the sharp edges of the geometry along the blade. Pressure gradient tend to increase on the polynomial convex side of the blade rather than the concave side facing the upstream caused by the tangential and normal forces of flowing wind. This may lead to structure properties issues and performance on the returning and advancing blades.

Generated result indicates high negative moments throughout the four revolutions of the three blades. The peak value for C_m is -0.25 and a total moment coefficient of -0.5 for the three blades. This results in low performance and negative C_p values. Negative instantaneous moments on advancing and returning blades cause the turbine to be motionless or moving back and forth relative to the wind speed. The reason is the scale of the turbine and low velocity wind speed with regards to the turbine size where it requires a large amount of drag force to rotate the blades. Hence it becomes difficult for the wind energy to initiate a rotation due to the large scale and dead weight.

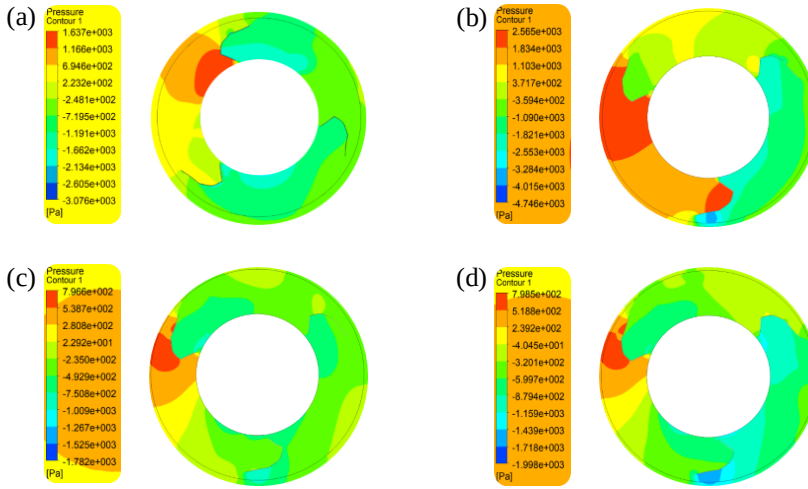

Figure 8: Static pressure contour for four different angles (a) 24°, (b) 360°, (c) 720° and (d) 1080°.

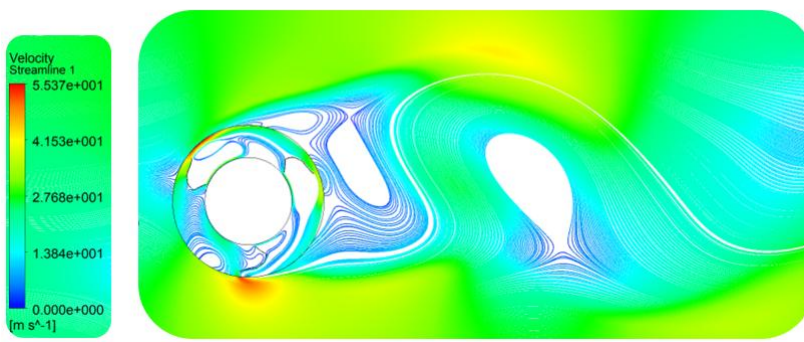

Figure 9: Streamline countor at 1440°.

Conclusion

This paper presented the fundamental aerodynamic study of a new WT design at preliminary stage. Based on the 2D unsteady numerical study, the effect of flow field properties on the performance of WT has been scrutinized. Under the numerical and design configuration the blade achieves a negative moment in initial cycle. It is observed that the sharp corners of the

cavity vane are responsible for rise in static pressure. Hence altering geometry of the cavity vane by means of making the profile more streamline prevents the returning blade affecting the motion of advancing blade. Design modification on overall structure will reduce the intensity of wake and vortex shedding on the proposed design. Advancing blade moment generation is overwhelmed by high average static pressure of 64.8 kPa exerted on the returning blade 1. Blade 1-3 indicated stable numerical values after 216°.

Acknowledgment

This research work was conducted under the Fundamental Research Grant Scheme no. FRGS/1/2019/TK10/UMP/02/4. We thank UMP for providing the computing resources.

References

[1] N. Qin, R. Howell, N. Durrani, K. Hamada, and T. Smith, "Unsteady Flow Simulation and Dynamic Stall Behaviour of Vertical Axis Wind Turbine Blades," *Wind Engineering*, vol. 35, no. 4, pp 511–527, 2011.

[2] A. Bianchini, F. Balduzzi, P. Bachant, G. Ferrara, and L. Ferrari, "Effectiveness of two-dimensional CFD simulations for Darrieus VAWTs: a combined numerical and experimental assessment," *Energy Convers. Manag.*, vol. 136, pp 318–328, 2017.

[3] M. Daaboul and N. Saba, "Optimization of a Vertical Axis Wind Turbine Using FEA , Multibody Dynamics and Wind Tunnel Testing," in *7th Australasians Hydraulics and Fluid Mechanics Conference*, Brisbane, 2016, no. 6 R.A.R Enoggera QueenLand, pp 1–21.

[4] E. Möllerström, F. Ottermo, J. Hylander, and H. Bernhoff, "Noise Emission of a 200 kW Vertical Axis Wind Turbine," *Energies*, vol. 9, no. 1, pp. 19, 2015.

[5] T. F. Ishugah, Y. Li, R. Z. Wang, and J. K. Kiplagat, "Advances in wind energy resource exploitation in urban environment: A review," *Renew. Sustain. Energy Rev.*, vol. 37, pp 613–626, 2014.

[6] R. Nobile, M. Vahdati, J. F. Barlow, and A. Mewburn-Crook, "Unsteady flow simulation of a vertical axis augmented wind turbine: A two-dimensional study," *J. Wind Eng. Ind. Aerodyn.*, vol. 125, pp 168–179, 2014.

[7] S. Mekhilef, A. Safari, and D. Chandrasegaran, "Feasibility study of off-shore wind farms in Malaysia," *Energy Educ. Sci. Technol. Part A Energy Sci. Res.*, vol. 29, no. 1, pp 519–530, 2012.

[8] L.-W. Ho, "Wind energy in Malaysia: Past, present and future," *Renew. Sustain. Energy Rev.*, vol. 53, pp 279–295, 2016.

[9] N. F. Salleh, B. C. Chew, and S. R. Hamid, "Feasible application of

offshore wind turbines in Labuan Island, Sabah for energy complementary," in *AIP Conference Proceedings*, vol. 1818, pp 020047, 2017.
[10] A. Albani, M. Z. Ibrahim, and K. H. Yong, "The Feasibility Study of Offshore Wind Energy Potential in Kijal, Malaysia: The New Alternative Energy Source Exploration in Malaysia," *Energy Explor. Exploit.*, vol. 32, no. 2, pp 329–344, 2014.
[11] N. Siti Khadijah, Z. Azami, R. Ahmad Mahir, Z. Mohd Said, I. Kamarulzaman, and S. Kamaruzzaman, "Analyzing the East Coast Malaysia Wind Speed Data," *Int. J. Energy Environ.*, vol. 3, no. 2, 2009.
[12] A. A. Ahmad Zaman, F. E. Hashim, and O. Yaakob, "Satellite-Based Offshore Wind Energy Resource Mapping in Malaysia," *J. Mar. Sci. Appl.*, vol. 18, no. 1, pp 114–121, 2019.
[13] F. J. Fakaruddin, Y. W. Sang, M. K. Mat Adam, N. K. Chang, and M. H. Abdullah, "Analysis of the Northeast Monsoon 2016/2017," *Research Publication No. 1/2017, Malaysian Meteorological Department*, 2017.
[14] E. L. Petersen, "In search of the wind energy potential," *J. Renew. Sustain. Energy*, vol. 9, no. 5, pp 052301, 2017.
[15] A. A. Osinowo, X. Lin, D. Zhao, and K. Zheng, "On the Wind Energy Resource and Its Trend in the East China Sea," *J. Renew. Energy*, 2017, pp 1–14, 2017.
[16] J. Hart, "Comparison of Turbulence Modeling Approaches to the Simulation of a Dimpled Sphere," *Procedia Eng.*, 147, pp 68–73, 2016.
[17] S. Ashwindran, A. A. Azizuddin, and A. N. Oumer, "Computational fluid dynamic (CFD) of vertical-axis wind turbine: mesh and time-step sensitivity study," *J. Mech. Eng. Sci.*, vol. 13, no. 3, 2019.
[18] S. N. Ashwindran, A. A. Aziz, and A. N. Oumer, "A Rudimentary Computational Assessment of Low Tip Speed Ratio Asymmetrical Wind Turbine Blades," *Int. J. Integr. Eng.*, vol. 12, no. 4, 2020.
[19] R. Ramponi and B. Blocken, "CFD simulation of cross-ventilation flow for different isolated building configurations: Validation with wind tunnel measurements and analysis of physical and numerical diffusion effects," *J. Wind Eng. Ind. Aerodyn.*, 104–106, pp 408–418, 2012.
[20] B. K. Kirke and L. Lazauskas, "Enhancing the Performance of Vertical Axis Wind Turbine Using a Simple Variable Pitch System," *Wind Engineering*, vol. 15, no. 4, pp 187–195, 1991.
[21] A. M. Zemamou, "Review of savonius wind turbine design and performance," *Energy Procedia*, vol. 141, pp 383–388, 2017.